Low-Density Parity-Check (LDPC) Coded OFDM Systems with M-PSK

Hisashi Futaki † Tomoaki Ohtsuki ‡

†Graduate School of Science and Technology, Tokyo University of Science
‡Faculty of Science and Technology, Tokyo University of Science
2641 Yamazaki, Noda, Chiba 278-8510 Japan
E-mail : †j7301653@ed.noda.sut.ac.jp, †ohtsuki@ee.noda.sut.ac.jp

Abstract— **Orthogonal Frequency Division Multiplexing (OFDM) is a very attractive technique to achieve the high-bit-rate transmission required for the future mobile communications. To improve the error rate performance of OFDM, forward error correction coding is essential. Recently, low-density parity-check (LDPC) codes, which can achieve the near Shannon limit performance, have attracted much attention. We proposed the LDPC coded OFDM (LDPC-COFDM) systems to improve the error rate performance of OFDM [1]. We showed that LDPC codes are effective to improve the error rate performance of OFDM on a frequency-selective fading channel. In mobile communications the high bandwidth efficiency is required, and thus the multilevel modulation is preferred. In [2], we proposed the decoding algorithm for the LDPC-COFDM systems with M-PSK on an AWGN channel. In this paper, we evaluate the error rate performance of the LDPC-COFDM systems with M-PSK using the Gray and the natural mappings on an AWGN channel, and that of the systems with M-PSK using the Gray mapping on a flat Rayleigh fading channel. We show that the LDPC-COFDM systems with M-PSK using the Gray mapping have better error rate performance than the systems using the natural mapping on an AWGN channel. We also show that the LDPC-COFDM systems with QPSK is more effective than the other systems on a flat Rayleigh fading channel.**

I. Introduction

Orthogonal Frequency Division Multiplexing (OFDM) is a very attractive technique to achieve the high-bit-rate data transmission required for the future mobile communications. The OFDM system divides the wide signal bandwidth into many narrowband subchannels that are transmitted in parallel. To improve the error rate performance of OFDM, forward-error correction coding is essential. Many error-correcting codes have been applied to OFDM, convolutional codes, Reed-Solomon codes, Turbo codes [3], and so on.

Recently, low-density parity-check (LDPC) codes have attracted much attention particularly in the field of coding theory. LDPC codes were proposed by Gallager in 1962 [4][5] and the performance is very close to the Shannon limit with practical decoding complexity like Turbo codes. LDPC codes have been applied to BPSK on an additive white Gaussian noise (AWGN) and a Rayleigh fading channels [6]. LDPC codes have been also applied to 8PSK on an AWGN channel [7]. The error rate performance of LDPC codes has been evaluated on a block fading channel, and it has been shown that the LDPC codes achieve a large gain with respect to convolutional codes for the large packet length [8].

We proposed the LDPC coded OFDM (LDPC-COFDM) systems to improve the error rate performance of OFDM [1]. We showed that the LDPC-COFDM systems achieve the good error rate performance with a small number of iterations on both an AWGN and a frequency-selective fading channels [2]. Moreover, we showed that when E_b/N_0 is not so small and the block lengths of both LDPC and Turbo codes are almost the same, the LDPC-COFDM systems have better error rate performance than the Turbo coded OFDM (TCOFDM) systems on both an AWGN and a frequency-selective fading channels. In mobile communications, the high bandwidth efficiency is required, and thus the multilevel modulation is preferred. We proposed the decoding algorithm for the LDPC-COFDM systems with M-PSK and showed that it works correctly on an AWGN channel [2].

In this paper, we evaluate the bit error rate (BER) of the LDPC-COFDM systems with M-PSK using the Gray and the natural mappings on an AWGN channel. Note that in [2], we confirmed that the proposed decoding algorithm for the LDPC-COFDM systems with M-PSK works correctly only on an AWGN channel. Therefore, we also evaluate the error rate performance of the LDPC-COFDM systems with M-PSK using the Gray mapping on a flat Rayleigh fading channel. We show that the LDPC-COFDM systems with M-PSK using the Gray mapping have better BER than the systems using the natural mapping. We also show that on a slow fading channel, the error rate performance of the LDPC-COFDM systems with QPSK is almost identical to that of the systems with BPSK, while that of the systems with QPSK is slightly worse than that of the systems with BPSK on a fast fading channel. We also show that the error rate performance of the LDPC-COFDM systems with 8PSK is worse than that of the systems with BPSK, and as the fading rate becomes faster, the difference of the error rate performance between the LDPC-COFDM systems with BPSK and the systems with 8PSK becomes larger. From the results of our simulation, we can say that the LDPC-COFDM systems with QPSK is more effective than the other systems on a flat Rayleigh fading channel.

II. LDPC Code

LDPC codes and their iterative decoding algorithm were proposed by Gallager in 1962 [4][5]. LDPC codes have been almost forgotten for about thirty years, in spite of their excellent properties. However, LDPC codes are now recognized as good error-correcting codes achieving the near Shannon limit performance [9]. LDPC codes are linear block codes speci-

0-7803-7484-3/02/$17.00

fied by a sparse parity-check matrix with the number of 1's per column (column weight) and the number of 1's per row (row weight), both of which are very small compared to the block length [10]. LDPC codes are classified into two groups, regular LDPC codes and irregular LDPC codes. Regular LDPC codes have a uniform column weight and row weight, and irregular LDPC codes have a nonuniform column weight. Irregular LDPC codes have better performance than regular LDPC codes. Furthermore, when the block length is relatively large (more than 1000), irregular LDPC codes outperform Turbo codes [11]. We describe an LDPC code defined by $M \times N$ parity-check matrix $\mathbf{H}$ as (N,K) LDPC, where $K{=}N{-}M$ and the code rate is $R = K/N$. When the $\mathbf{H}$ doesn't have full rank, $K > N{-}M$ and the error rate performance of an LDPC code becomes worse. Thus, when we construct the parity-check matrix $\mathbf{H}$, we ensure that all the rows of the matrix are linearly independent.

LDPC codes can be decoded by using a probability propagation algorithm known as the sum-product or belief propagation algorithm [5][9], which is implemented by using a Factor Graph that contains two types of nodes: the "bit nodes" and the "check nodes" [12]. Each bit node corresponds to a column of a parity-check matrix, which also corresponds to a bit in the codeword. Each check node corresponds to a row of a parity-check matrix, which represents a parity-check equation. An edge between a bit node and a check node exists if and only if the bit participates in the parity-check equation. LDPC codes have better block error performance than Turbo codes, because the minimum distance of an LDPC code increases proportional to the code length with a high probability. Such a property is desirable for the high-bit-rate transmission that requires very low frame error probability.

III. Sum-product algorithm

First, we describe the notations of the sum-product algorithm in Fig. 1 (b). $\mathcal{M}(l)$ denotes the set of check nodes that are connected to the bit node l, i.e., positions of "1"s in the lth column of the parity-check matrix. $\mathcal{L}(m)$ denotes the set of bits that participates in the mth parity-check equation, i.e., the positions of "1"s in the mth row of the parity-check matrix. $q^i_{l\to m}$, where $i = 0, 1$, denotes the probability information that the bit node l sends to the check node m, indicating $P(x_l = i)$. $r^i_{m\to l}$ denotes the probability information that the mth check node gathers for the lth bit being i. The *a posteriori* probability for a bit is calculated by gathering all the extrinsic information from the

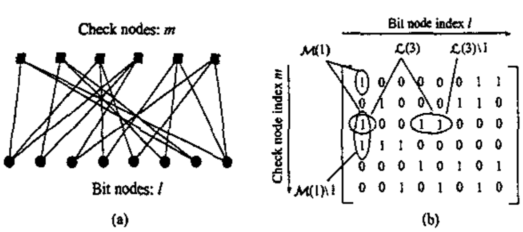

Fig. 1. (a) Factor graph and (b) notation for sum-product algorithm

check nodes that connect to it, which can be obtained by the following iterative belief propagation procedure.

For binary codes, the sum-product algorithm can be performed more efficiently in Log domain, where the probabilities are equivalently characterized by the log-likelihood ratios (LLRs): $L(r_{m\to l}) \triangleq \log(r^1_{m\to l}/r^0_{m\to l})$, $L(q_{m\to l}) \triangleq \log(q^1_{m\to l}/q^0_{m\to l})$, $L(p_l) \triangleq \log(p^1_l/p^0_l)$, $L(q_l) \triangleq \log(q^1_l/q^0_l)$. Note that p^i_l represents the likelihood that the lth bit is i.

Initialization

Each bit node l is assigned an *a priori* LLR $L(p_l)$. In the case of equiprobable inputs on a memoryless AWGN channel with BPSK,

$$L(p_l) = \log \frac{P(y_l \,|\, x_l = +1)}{P(y_l \,|\, x_l = -1)} = \frac{2}{\sigma^2} y_l$$

where x, y represent the transmitted bit and received bit, respectively, and σ^2 is the noise variance. For every position (m, l) such that $H_{ml} = 1$, where H_{ml} represents the element of the mth row and the lth column in the parity-check matrix $\mathbf{H}$, $L(q_{l\to m})$ and $L(r_{m\to l})$ are initialized as:

$$L(q_{l\to m}) = L(p_l) \quad \text{and} \quad L(r_{m\to l}) = 0$$

L1. Checks to bits

Each check node m gathers all the incoming information $L(q_{l\to m})$'s, and updates the belief on the bit l based on the information from all other bits connected to the check node m.

$$L(r_{m\to l}) = 2\tanh^{-1}\left(\prod_{l' \in \mathcal{L}(m)\backslash l} \tanh(L(q_{l'\to m})/2)\right)$$

L2. Bits to checks

Each bit node l propagates its probability to all the check nodes that connect to it.

$$L(q_{l\to m}) = L(p_l) + \sum_{m' \in \mathcal{M}(l)\backslash m} L(r_{m'\to l})$$

L3. Check stop criterion

The decoder obtains the total *a posteriori* probability for the bit l by summing the information from all the check nodes that connect to the bit l.

$$L(q_l) = L(p_l) + \sum_{m \in \mathcal{M}(l)} L(r_{m\to l})$$

Hard decision is made on the $L(q_l)$, and the resulting decoded input $\hat{\mathbf{x}}$ is checked against the parity-check matrix $\mathbf{H}$. If $\mathbf{H}\hat{\mathbf{x}} = \mathbf{0}$, the decoder stops and outputs $\hat{\mathbf{x}}$. Otherwise, it repeats the steps L1–L3. The sum-product algorithm sets the maximum number of iterations. If the number of iterations becomes the maximum number of iterations, the decoder stops and outputs $\hat{\mathbf{x}}$ as the results of the hard decision.

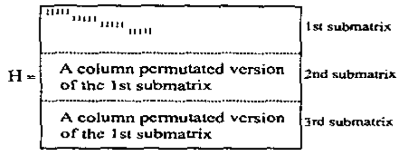

Fig. 2. Construction of an LDPC code

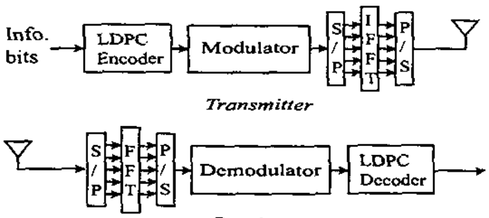

Fig. 3. LDPC-COFDM system model

IV. LDPC Coded OFDM

A. Construction of LDPC Code

Fig. 2 shows the way to construct an LDPC code in this paper, which is depicted in [4]. A parity-check matrix is divided into three submatrices, each containing a single 1 in each column. The first of these submatrices contains 1's in descending order; i.e., the ith row contains 1's in the columns $(i-1)k+1$ to ik, where k is the row weight. The other submatrices are merely column permutations of the first submatrix. The permutations of the 2nd submatrix and the 3rd submatrix are independently selected. After constructing the parity-check codes like this, we remove the 4-cycle from the parity-check matrix by extracting the corresponding columns.

B. System Model

In a multipath fading channel, some subcarriers of OFDM may be completely lost because of the deep fades. Hence, in this case, it is expected that lots of errors fix on continuous some subcarriers and the two dimensional errors in time and frequency domains occur. That is why we apply LDPC codes, which can compensate for the two dimensional errors, to OFDM system.

Fig. 3 shows the model of the LDPC-COFDM system. At the transmitter, information bits are encoded at the LDPC encoder and modulated at the modulator. After the serial-to-parallel conversion, the OFDM sub-channel modulation is implemented by using an inverse fast Fourier transform (IFFT) and the outputs of the IFFT are assigned to some OFDM symbols for the purpose of compensating two dimensional errors in the OFDM system. At the receiver, after the serial-to-parallel conversion, the OFDM sub-channel demodulation is implemented by using a fast Fourier transform (FFT). The received OFDM symbols generated by the FFT are demodulated at the demodulator. The demodulated bits are decoded with each LDPC encoded block and data bits are restored.

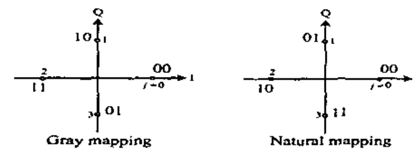

Fig. 4. QPSK mapping

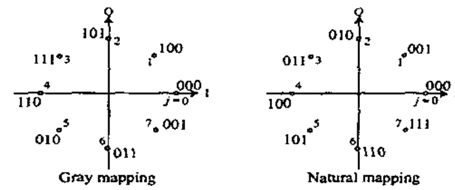

Fig. 5. 8PSK mapping

C. Decoding Algorithm for M-PSK

We explain the bit-wise sum-product algorithm for the LDPC-COFDM systems with M-PSK. We initialize the first likelihood of the received signal as follows. We define the first likelihood corresponding to the tth bit of the sth received symbol as:

$$L(p_{s,t}) = \frac{P(\boldsymbol{y}_s \mid x_l = 1)}{P(\boldsymbol{y}_s \mid x_l = 0)} = \frac{\sum_{j \in \{\boldsymbol{J}_{t,1}\}} \exp\left[-\frac{(y_{s,I} - x_{I,j})^2 + (y_{s,Q} - x_{Q,j})^2}{2\sigma^2}\right]}{\sum_{j \in \{\boldsymbol{J}_{t,0}\}} \exp\left[-\frac{(y_{s,I} - x_{I,j})^2 + (y_{s,Q} - x_{Q,j})^2}{2\sigma^2}\right]}$$

where $x_l, \boldsymbol{y}_s$ represent the lth transmitted bit and the sth received symbol, respectively, and $\boldsymbol{J}_{t,i}$ represents the set of M-PSK symbols with the tth bit being i. In the case of the QPSK, we initialize the first likelihood of the received signal as:

$$L(p_l) = \begin{cases} L(p_{s,1}), & (l = 2s-1) \\ L(p_{s,2}), & (l = 2s) \end{cases}$$

In the case of the 8PSK, we initialize the first likelihood of the received signal as:

$$L(p_l) = \begin{cases} L(p_{s,1}), & (l = 3s-2) \\ L(p_{s,2}), & (l = 3s-1) \\ L(p_{s,3}), & (l = 3s) \end{cases}$$

After initializing the likelihood of the received signal like this, the decoding is done in the same procedure as for BPSK, L1–L3.

V. Simulation Results

We present some results of our computer simulation. TABLE I shows the simulation parameters. We use the (1080,525) LDPC code with column weight of 3 and set the maximum number of iterations in decoding to 100.

TABLE I

SIMULATION PARAMETERS

Modulation	BPSK, QPSK, 8PSK
Amplifier	Linear
Number of subcarriers	64
Number of FFT points	512
Channel models	AWGN Flat Rayleigh fading
Bandwidth	40 MHz
Maximum Doppler frequency	5, 80, 1000 Hz

Fig. 6 shows the BERs of the LDPC-COFDM systems with M-PSK using Gray and natural mappings on an AWGN channel. We can see that the BER of the LDPC-COFDM systems with QPSK using Gray mapping is about 1.2 dB better than that of the systems with QPSK using natural mapping. This is because the Hamming distance between the adjacent symbols of Gray mapping is smaller than that of natural mapping. We can also see that the BER of the LDPC-COFDM systems with QPSK using Gray mapping is almost identical to that of the systems with BPSK. We can also see that the BER of the LDPC-COFDM systems with 8PSK using Gray mapping is about 3 dB better than that of the systems with 8PSK using natural mapping. Moreover, the BER of the LDPC-COFDM systems with 8PSK using Gray mapping is about 1.3 dB worse than that of the systems with BPSK. Note that, the BER of the uncoded system with 8PSK, that is not shown in this figure, is about 3 dB worse than that of the uncoded system with BPSK. Considering the bandwidth efficiency, we can say that the LDPC-COFDM systems with 8PSK using Gray mapping is attractive than the systems with BPSK on an AWGN channel.

Fig. 7 ~ 9 show the BER and the OFDM symbol error rate (SER) of the LDPC-COFDM systems with M-PSK using Gray mapping on a flat Rayleigh fading channel, where the maximum Doppler frequency is f_d = 5, 80, 1000 Hz, respectively. In Fig. 7, we can see that the error rate performances of the LDPC-COFDM systems with BPSK and QPSK are almost identical, while the error rate performance of the systems with 8PSK is about 1.5 dB worse than that of the systems with BPSK or QPSK. Comparing the error rate performances of the LDPC-COFDM systems on an AWGN and a slow fading channels (f_d = 5 Hz), the difference of the error rate performances between the systems with BPSK and the systems with M-PSK is almost identical. Note that on a slow fading channel, the BERs of the uncoded systems with QPSK and 8PSK, that are not shown in this figure, are about 0.5 and 5 dB worse than that of the uncoded systems with BPSK, respectively. In Fig. 8, we can see that the error rate performance of the LDPC-COFDM systems with QPSK is slightly worse than that of the systems with BPSK, while that of the LDPC-COFDM systems with 8PSK is about 3 dB worse than that of the systems with BPSK. Compared with the error rate performances on a slow fading channel, since the LDPC-COFDM systems with 8PSK are more influenced by the Doppler spread, the difference of the error rate performances between the systems with BPSK and the systems with 8PSK is large on a fast fading channel (f_d = 80 Hz). In Fig. 9, we can see that the error rate performances of the LDPC-COFDM systems with QPSK and 8PSK are 0.5 dB and 3.5 dB worse than that of the systems with BPSK, respectively. Note that on a fast fading channel (f_d = 1000 Hz), the BER of the uncoded systems with QPSK is about 3 dB worse than that of the uncoded systems with BPSK. Note that the uncoded systems with 8PSK have the error floor at BER of 10^{-2}.

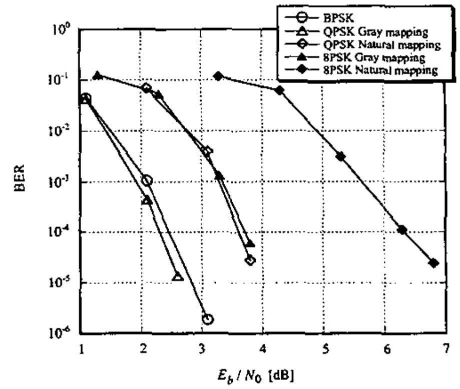

Fig. 6. BER of the (1080,525) LDPC-COFDM systems with M-PSK using Gray and natural mappings on an AWGN channel

Fig. 10 shows the required E_b/N_0 for the BER of 10^{-4} versus the normalized Doppler frequency f_dNT_s for the (1080,525) LDPC-COFDM systems with M-PSK on a flat Rayleigh fading channel. Here, f_d denotes the maximum Doppler frequency and T_s denotes the OFDM symbol-duration. We can see that as the normalized Doppler frequency f_dNT_s becomes higher, the required E_b/N_0 for the LDPC-COFDM systems becomes larger. For instance, when the $f_dNT_s = 6.40 \times 10^{-5}$ (slow fading channel), the required E_b/N_0 for the LDPC-COFDM systems with BPSK, QPSK, 8PSK are about 2.2, 2.25, 3.7 dB, respectively. When the $f_dNT_s = 1.28 \times 10^{-2}$ (fast fading channel), the required E_b/N_0 for the systems with BPSK, QPSK, 8PSK are about 3.5, 3.9, 6.9 dB, respectively. Note that the increase of the required E_b/N_0 for the systems with 8PSK is larger than that for the systems with BPSK or QPSK. From these results, we can say that the LDPC-COFDM systems with QPSK using Gray mapping is more effective than the other systems on a flat Rayleigh fading channel.

VI. CONCLUSIONS

In this paper, we evaluated the error rate performance of the (1080,525) LDPC-COFDM systems with M-PSK on both an AWGN and a flat Rayleigh fading channels. We showed that the LDPC-COFDM systems with M-PSK using Gray mapping have the better error rate performance than the systems with M-PSK using natural mapping on an AWGN channel. Considering the bandwidth efficiency, we can say that the LDPC-COFDM systems with 8PSK using Gray mapping is attractive than the systems with BPSK on an AWGN channel. We also showed that on a slow fading channel, the error rate performance of the LDPC-COFDM systems with QPSK using Gray mapping is al-

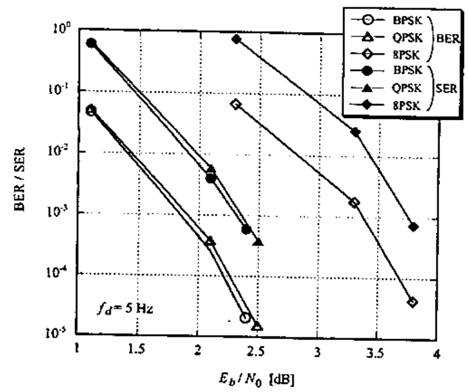

Fig. 7. BER/SER of the (1080,525) LDPC-COFDM with M-PSK using Gray mapping on a flat Rayleigh fading channel. $f_d = 5$ Hz

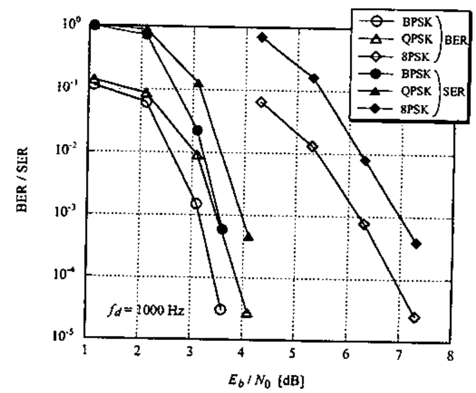

Fig. 9. BER/SER of the (1080,525) LDPC-COFDM with M-PSK using Gray mapping on a flat Rayleigh fading channel. $f_d = 1000$ Hz

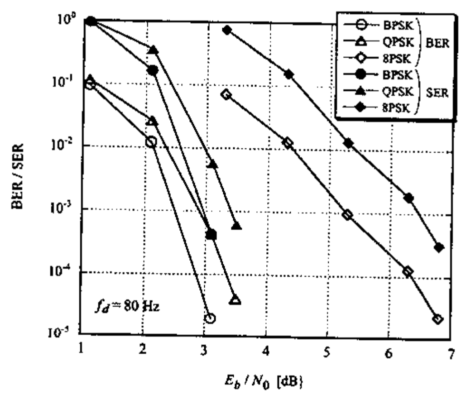

Fig. 8. BER/SER of the (1080,525) LDPC-COFDM with M-PSK using Gray mapping on a flat Rayleigh fading channel. $f_d = 80$ Hz

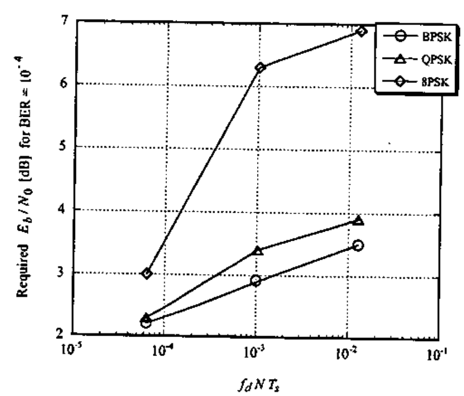

Fig. 10. Required E_b/N_0 for the BER of 10^{-4} versus the normalized Doppler frequency $f_d N T_s$ for the (1080,525) LDPC-COFDM with M-PSK using Gray mapping on a flat Rayleigh fading channel

most identical to that of the systems with BPSK, while that of the systems with 8PSK is about 0.8 dB worse than that of the systems with BPSK. We also showed that as the $f_d N T_s$ becomes higher, the required E_b/N_0 for the LDPC-COFDM systems, particularly for the systems with 8PSK, becomes larger. Thus, we can say that the LDPC-COFDM systems with QPSK using Gray mapping is more effective than the other systems on a flat Rayleigh fading channel.

References

[1] H. Futaki and T. Ohtsuki, "Low-density parity-check (LDPC) coded OFDM systems," *IEEE VTC2001 fall*, vol. 1, pp. 82 – 86, Oct. 2001.

[2] H. Futaki and T. Ohtsuki, "Performance of low-density parity-check coded OFDM systems," *IEEE ICC2002*, (to appear).

[3] C. Berrou and A. Glavieux, "Near optimum error correcting coding and decoding: Turbo-codes," *IEEE. Trans. Commun.*, vol. 44, no. 10, pp. 1261 – 1271 Oct. 1996.

[4] R. G. Gallager, "Low density parity check codes," *IRE Trans. Inform. Theory*, vol. IT – 8, pp. 21 – 28, Jan. 1962.

[5] R. G. Gallager, *Low Density Parity Check Codes*, no. 21 in Research Monograph Series. Cambridge, MA: MIT Press, 1963

[6] J. Hou, P. H. Siegel, and L. B. Milstein, "Performance analysis and code optimization of low density parity-check codes on Rayleigh fading channels," *IEEE JSAC*, vol. 19, no.5, pp. 924 – 934, May. 2001.

[7] T. Wadayama, "A coded modulation scheme based on low density parity check codes," The 23rd SITA 2000, pp. 379 – 382, Oct. 2000.

[8] M. Chiani, A. Conti and A. Ventura, "Evaluation of low-density parity-check codes over block fading channels" *IEEE. ICC'2000*, vol.3, pp. 1183 – 1187, 2000.

[9] D. J. C. MacKay and R. M. Neal, "Near Shannon limit performance of low density parity check codes," *Electron. Lett.*, vol. 32, no. 18, pp. 1645 – 1646, Aug. 1996.

[10] D. J. C. MacKay, "Good error-correcting codes based on very sparse matrices," *IEEE Trans. Inform. Theory*, vol. 45, pp. 399 – 431, Mar. 1999.

[11] T. Richardson, A. Shokrollahi and R. Urbanke, "Design of provably good low-density parity-check codes," submitted to *IEEE Trans. Inform. Theory*.

[12] F. R. Kschischang, B. J. Frey and H. A. Loeliger, "Factor graphs and the sum-product algorithm," *IEEE. Trans. Inform. Theory*, vol.47, no. 2, pp. 498 – 519, Feb. 2001.

[13] Y. Kou, S. Lin and M. P. C. Fossorier, "Low density parity check codes: construction based on finite geometries," *IEEE GLOBECOM'2000*, vol.2, pp. 825 – 829, 2000.

[14] D. Hösli, E. Svensson and D. Arnold, "High-rate low-density parity-check codes: construction and application," *2nd International Symposium on Turbo Codes*, pp. 447 – 450, 2000.